



OPEN ACCESS

EDITED BY

Paola Perin,
University of Pavia, Italy

REVIEWED BY

Helge Rask-Andersen,
Uppsala University, Sweden
Benjamin J. Seicol,
The Ohio State University, United States

*CORRESPONDENCE

Hainan Lang
✉ langh@muscc.edu

[†]These authors have contributed equally to this work

RECEIVED 29 April 2023

ACCEPTED 05 July 2023

PUBLISHED 25 July 2023

CITATION

Brown LN, Barth JL, Jafri S, Rumschlag JA, Jenkins TR, Atkinson C and Lang H (2023) Complement factor B is essential for the proper function of the peripheral auditory system. *Front. Neurol.* 14:1214408. doi: 10.3389/fneur.2023.1214408

COPYRIGHT

© 2023 Brown, Barth, Jafri, Rumschlag, Jenkins, Atkinson and Lang. This is an open-access article distributed under the terms of the [Creative Commons Attribution License \(CC BY\)](https://creativecommons.org/licenses/by/4.0/). The use, distribution or reproduction in other forums is permitted, provided the original author(s) and the copyright owner(s) are credited and that the original publication in this journal is cited, in accordance with accepted academic practice. No use, distribution or reproduction is permitted which does not comply with these terms.

Complement factor B is essential for the proper function of the peripheral auditory system

LaShardai N. Brown^{1†}, Jeremy L. Barth^{2†}, Shabih Jafri^{1†}, Jeffrey A. Rumschlag¹, Tyreek R. Jenkins¹, Carl Atkinson³ and Hainan Lang^{1*}

¹Department of Pathology and Laboratory Medicine, Medical University of South Carolina, Charleston, SC, United States, ²Department of Regenerative Medicine and Cell Biology, Medical University of South Carolina, Charleston, SC, United States, ³Division of Pulmonary Medicine, University of Florida, Gainesville, FL, United States

Sensorineural hearing loss is associated with dysfunction of cochlear cells. Although immune cells play a critical role in maintaining the inner ear microenvironment, the precise immune-related molecular mechanisms underlying the pathophysiology of hearing loss remain unclear. The complement cascade contributes to the regulation of immune cell activity. Additionally, activation of the complement cascade can lead to the cellular opsonization of cells and pathogens, resulting in their engulfment and elimination by phagocytes. Complement factor B (fB) is an essential activator protein in the alternative complement pathway, and variations in the fB gene are associated with age-related macular degeneration. Here we show that mice of both sexes deficient in fB functional alleles (fB^{-/-}) demonstrate progressive hearing impairment. Transcriptomic analysis of auditory nerves from adult mice detected 706 genes that were significantly differentially expressed between fB^{-/-} and wild-type control animals, including genes related to the extracellular matrix and neural development processes. Additionally, a subset of differentially expressed genes was related to myelin function and neural crest development. Histological and immunohistochemical investigations revealed pathological alterations in auditory nerve myelin sheathes of fB^{-/-} mice. Pathological alterations were also seen in the stria vascularis of the cochlear lateral wall in these mice. Our results implicate fB as an integral regulator of myelin maintenance and stria vascularis integrity, underscoring the importance of understanding the involvement of immune signaling pathways in sensorineural hearing loss.

KEYWORDS

cochlea, complement factor B, macrophage, auditory nerve, glial cell, myelination, stria vascularis, hearing loss

1. Introduction

Sensorineural hearing loss (SNHL) is a multifactorial disorder resulting from dysfunction of cochlear structures. Despite the growing prevalence of SNHL worldwide (1), the pathological mechanisms underlying SNHL remain elusive. Recent findings highlight the important role of inflammation, pro-inflammatory mediators, and dysregulation of the immune system in exacerbating cellular degeneration in neurological disorders including age-related hearing loss (2–4). Dysregulation of the complement signaling pathways may contribute to age-related

pathological alterations in the brain and neurological disorders (5). The complement pathway has been associated with several cellular processes in the central nervous system, including synaptic plasticity and synaptic pruning during development (6, 7), axonal pruning [e.g., via microglial trophocytosis; (8)], and blood-brain barrier mediation (9). Complement signaling has also been found to contribute to neurodegenerative pathologies, including multiple sclerosis (10), drug-induced excitotoxicity (11), and Alzheimer's Disease (12). However, the impacts of the different complement pathways in healthy and impaired auditory systems are just beginning to be elucidated.

Complement signaling is comprised of over 50 fluid-phase and membrane-bound proteins that are important for activating the innate immune system. The complement cascade can be activated by 3 pathways: classical, lectin, and alternative pathways (13, 14). Recent studies have highlighted the potential role of classical complement signaling in auditory function. For instance, *C1ql1* is expressed in the outer hair cells of young adult mice (15) and global *C1ql1*-deficient mice show a decline in hearing sensitivity and pathological alterations in the auditory nerve and outer hair cells (15, 16). Additionally, levels of complement factor I (CFI, known as C3b/C4b inactivator) were increased in the sensory epithelium following noise trauma in a rodent model (17). These observations reveal a potential role for complement signaling in regulating the development and maintenance of cochlear structure and function.

Interestingly, the alternative pathway amplifies the activation of the classical and lectin pathways through the activity of complement factor B (fB). During spontaneous activation of the alternative pathway, fB binds to and cleaves C3 to generate C3b. Fragments of fB bind to C3b to catalyze the creation of the alternative pathway C3 convertase, C3bBb, which then amplifies complement activation and contributes to the formation of the membrane attack complex (13, 18). A previous study reported that fB was highly expressed in the middle ear epithelium following *Streptococcus pneumoniae* infection in rodent models of otitis media, demonstrating that alternative complement activation was essential for protection against otitis media (19). Here, we examined the role of alternative complement protein fB in the peripheral auditory system using a well-characterized mouse model of fB deficiency (fB^{-/-}) (20–22). Using a combination of auditory brainstem response (ABR) measurements, RNA-sequencing, electron microscopy ultrastructural analyses, and quantitative immunohistochemical investigations, our data revealed an important role for alternative complement signaling in the peripheral auditory system. We found that fB deficiency results in reduced hearing sensitivity and declines in auditory nerve function, along with significant alterations of auditory nerve myelin and defects in the interdigitation of cells in the stria vascularis of the cochlear lateral wall. These results suggest that the alternative complement pathway plays a role in regulating proper auditory function and the development and maintenance of the cochlear structure.

2. Materials and methods

2.1. Animals

CBA/CaJ and C57Bl/6J mice are established models for hearing research. Since C57Bl/6J mice maintain an *Ahl* gene mutation and exhibit early-onset age-related morphological alterations (23), CBA/

CaJ mice were used for the investigation of RNA profiling to explore complement-related expression in the developing cochlea. For analysis of complement-related gene expression in the developing cochlea, P3, P7, P14, and P21 CBA/CaJ mice of both sexes were used. CBA/CaJ mice, originally purchased from the Jackson Laboratory (Bar Harbor, ME), were bred in-house in a low-noise environment at the Animal Research Facility of the Medical University of South Carolina (MUSC; Charleston, SC, United States). Factor B deficient (fB^{-/-}) mice were established previously (20) and provided by Dr. Carl Atkinson. The model was generated by targeted homologous recombination in embryonic stem cells, resulting in mice with non-functional fB alleles. These mice show no gross difference in phenotype when compared to wild-type (WT, C57Bl/6J) mice. Young adult (1.5–4 months) WT and fB^{-/-} mice of both sexes were used in this study. All aspects of animal research were conducted in accordance with the guidelines of the Institutional Animal Care and Use Committee of MUSC (IACUC-2020-01132). All mice received food and water *ad libitum* and were maintained on a 12-h light/dark cycle.

2.2. Assessment of auditory functions

Auditory brainstem responses (ABR) were measured as previously described (24–26). Briefly, mice were anesthetized by intraperitoneal injection of xylazine (20 mg/kg) and ketamine (100 mg/kg) and placed in a sound-isolation room. Depth of anesthesia was regularly examined by lack of foot-pinch response. Using Tucker-Davis Technologies System III equipment (Tucker-Davis Technologies, Gainesville, FL, United States) and a SigGen software package (Version 4.4.1), acoustic stimuli were generated, and sound calibration was completed using an IPC Microphone System (PCB Piezotronics Inc., Depew, NY, United States). The acoustic stimuli were presented to the animal's ear canal through a 3–5 mm outer diameter plastic tube. Auditory function was assessed by evoking responses at half-octave frequencies from 4 kHz to 45.2 kHz with 5 ms duration tone pips, with 0.5 ms cos² rise/fall times, delivered at a rate of 31 times/s. Sound levels were reduced from 90 to 5 dB sound pressure level (SPL) in 5 dB SPL intervals. Hearing thresholds were identified as the lowest intensity that produced a reproducible response wave.

2.3. Immunohistochemistry and quantitative analysis

Cochleae were collected and fixed as described previously (24). Tissues were then embedded in Tissue-Tek OCT Compound (VWR, Radnor, PA, United States) and sectioned at 10 μm thickness. Tissues were washed with 10 mM PBS and permeabilized with 2% bovine serum albumin and 0.4% Triton X-100 (Sigma, Burlington, MA, United States) for 15 min. Sections were then blocked with normal goat serum solution for 1 h at room temperature and incubated overnight with primary antibodies at 4°C: rabbit anti-Iba1 [Wako Chemicals USA Inc., Richmond, VA, United States (1:250)], mouse anti-Neurofilament 200 [Sigma-Aldrich, Burlington, MA, United States (1:200)], rabbit anti-Myosin VIIa [Proteus BioSciences, Ramona, CA, United States (1:200)], goat anti-Sox10 [Santa Cruz Biotechnology, Santa Cruz, CA, United States (1:80)], rabbit

anti-Kir4.1 [Alomone, Jerusalem, Israel (1:200)] and mouse anti-Na,K-ATPase (α 1) [DSHB, Iowa City, IA, United States (1:50)]. Secondary antibodies were biotinylated and binding was detected by labeling with fluorescein (FITC)-conjugated avidin D, Texas Red-conjugated avidin D (Vector Labs, Burlingame, CA, United States) or Alexa Fluor Dyes (ThermoFisher Scientific, Waltham, MA, United States). Nuclei were counterstained with propidium iodide (PI).

Sections were examined with a Zeiss Axio Observer (Carl Zeiss Inc., Jena, Germany), and the captured images were processed using Image-Pro Plus software (Media Cybernetics, MD). Quantitative analysis was done using AxioVision 4.8.2 (Carl Zeiss, Inc., Jena, Germany) software. Regions of interest (ROI) in the auditory nerve section were defined using the software outline tool. Apical, middle, and basal portions of the cochleae were examined (27). Within each measured area (or ROI), total cell numbers were determined by counting PI counterstained cell nuclei using the software measurement tool. For quantitative analysis of strial intermediate cell function, cochlear frozen sections of $fB^{-/-}$ and wildtype mice were immunostained using Kir4.1 antibody, a marker of strial intermediate cells. After identifying the ROI, a grayscale was applied to the image using the Automatic Measurement Feature in Axiovision 4.8.2. This function allows for the accurate identification of fluorescent light and provides a means to quantitatively determine regions of Kir4.1 immunoreactivity. Subsequently, fluorescence density measurements were determined by calculating immunostaining intensity and dividing by the ROI area. Three to 7 slides were randomly selected from each cochlea and used for data collection. For the count of IBA1⁺ macrophages, only macrophages having at least one component with a diameter of more than 5 μ m or visible nuclei were counted. The method of statistical analysis is also described below.

2.4. Confocal microscopy

Sections were examined on a Zeiss LSM5 Pascal (Carl Zeiss Inc.) confocal microscope, a Zeiss LSM 880 NLO, or Leica TCS SP5 (Leica Microsystems, Allendale, NJ, United States) confocal microscope. FITC and Texas Red signals were detected by excitation with the 488 nm and 543 nm lines, respectively. Images were scanned at image scales of 225.0 μ m (x) \times 225.0 μ m (y), 144.72 μ m (x) \times 144.72 (y), and 450.0 μ m (x) \times 450.0 μ m (y). Captured images were processed using Zen 2012 Blue acquisition software (Carl Zeiss Inc.), Leica Application Suite X software (Version 3.0.2.16120), and Adobe Photoshop CS6 (Adobe Systems Inc., San Jose, CA, United States).

2.5. Transmission electron microscopy

Young adult and postnatal WT and $fB^{-/-}$ mice were used for electron microscopy analysis. These mice included 2 young adult WTs, 2 young adult $fB^{-/-}$ mice, 2 P14 WTs, 2 P14 $fB^{-/-}$ mice, 1 P16 WT, and 1 $fB^{-/-}$ mouse. Mice were anesthetized and perfused via a cardiac catheter with 10 mL of normal saline containing 0.1% sodium nitrite followed by 15 mL of a mixture of 4% paraformaldehyde and 2% glutaraldehyde in 0.1 M phosphate buffer, pH 7.4. Cochleae were removed and perfused through the oval window with approximately 3 mL of the fixative mixture. Inner ears were dissected and immersed in the fixative agent overnight at

4°C. Cochleae were decalcified by immersion in 40 mL of 120 mM solution of EDTA, pH 7.0, with gentle stirring at room temperature for 2–3 days with daily changes of the EDTA solution. Cochlear tissues were postfixed with 1% osmium tetroxide-1.5% ferrocyanide for 2 h in the dark, then dehydrated and embedded in Epon LX 112 resin. Ultrathin sections (70 nm thick) were stained with uranyl acetate and lead citrate and examined and imaged using a JEOL JEM-1010 transmission electron microscope (JEOL USA, Inc., Peabody, MA, United States). The middle portions of the cochleae were assessed for the structural integrity of the sensory hair cell, and cells in the auditory nerve and stria vascularis. Pathologies of the auditory nerve and stria vascularis were characterized using criteria outlined in previously published studies (25, 28, 29). The observer was not blinded to the genotype while assessing micrographs across each strain. For light microscopy of toluidine-blue stained sections, Epon-embedded sections with 1 μ m thickness were stained with 10% toluidine blue for 1 min, rinsed in H₂O, and allowed to air-dry overnight before imaging.

2.6. RNA isolation and sequencing

To examine the expression of complement-related genes in the developing cochlea, RNA profiling was performed on P3, P7, P14, and P21 CBA/CaJ mice. To examine the consequences of fB deficiency on RNA expression, young adult WT (C57BL/6J) and $fB^{-/-}$ mice were used. Auditory nerves of mice were isolated by microdissection of the modiolus from structures of the cochlear bulla, cochlear lateral wall, and sensory epithelium. Tissue collected from both cochleae of each mouse was pooled to make an individual sample. Total RNA was purified by miRNeasy Mini Kit (Qiagen Inc., Germantown, MD, United States) per manufacturer instructions. The quality of total RNA preparations was assessed by Agilent 2,100 Bioanalyzer; low-quality samples (RIN <7) were excluded from the study. Sequencing was done on three biological replicates ($n = 3$) of each sample type at the Medical University of South Carolina Genomics Resource. Libraries were prepared using standard Illumina protocols and the TruSeq RNA Library Prep Kit (Illumina Inc., San Diego, CA, United States). Samples were sequenced on an Illumina HiSeq 2,500. Sequencing data were analyzed using Partek® Flow® software (Partek Inc., St. Louis, MO, United States). Reads were aligned to mouse genome assembly mm10 by TopHat2 and quantified to an annotation model (Partek E/M) using mm10 with the following criteria: (a) strict paired-end compatibility, (b) junction reads to match introns required, (c) minimum read overlap with feature at 100% of reading length, and (d) minimum of 10 reads. Comparative analysis was done with DESeq2 (30). Differential expression for complement factor B deficiency was defined as an adjusted p -value (FDR step up) <0.05 and an absolute fold change >1.5. Biological process enrichment analysis was conducted with ToppGene (31). For the focused analysis of complement gene expression during AN development, a list of complement genes was compiled based on literature review and gene ontology information; differential expression of these genes was defined as adjusted p -value (FDR step up) <0.05 for at least one pairwise relationship. Raw sequencing data (fastq files) and comparison results are archived in NCBI Gene Expression Omnibus (Complement Factor B study, accession GSE182417; Developmental study, GSE133823).

2.7. Statistical analysis

For analyses apart from RNAseq, quantitative data are expressed as mean \pm SEM, unless otherwise specified. For ABR thresholds, latencies, and wave I amplitudes, linear mixed-effects regression (LMER) models were fit and analyzed using R language [version 4.0.5; R Core Team (2021) and *lme4* package (32)]. LMER is a non-parametric statistical approach that can test hypothesis-driven relationships between predictor and outcome variables while accounting for random variation within and between groups. The interaction models for thresholds included fixed effects of genotype, age, and stimulus frequency, with a random effect of the mouse identification number. Interaction models for latencies and amplitudes included fixed effects of genotype, age, and sound level, with a random effect of the mouse identification number. Type III ANOVA [*car* package; (33)] was run on the LMER models. Degrees of freedom were estimated using the Satterthwaite approximation and rounded to the nearest whole number. *Post-hoc* pairwise comparisons were conducted using the *emmeans* package (34) to obtain estimated marginal means and contrasts, adjusting for multiple comparisons using the Tukey method. Neuron and macrophage count data and Kir4.1 immunofluorescence measure data were analyzed using GraphPad Prism 7 software (GraphPad Software, Inc. La Jolla, CA) for Windows and significance was determined by Mann-Whitney U test. For all statistical tests, a *p*-value of ≤ 0.05 was considered significant. The sample size is indicated in each figure or figure legend.

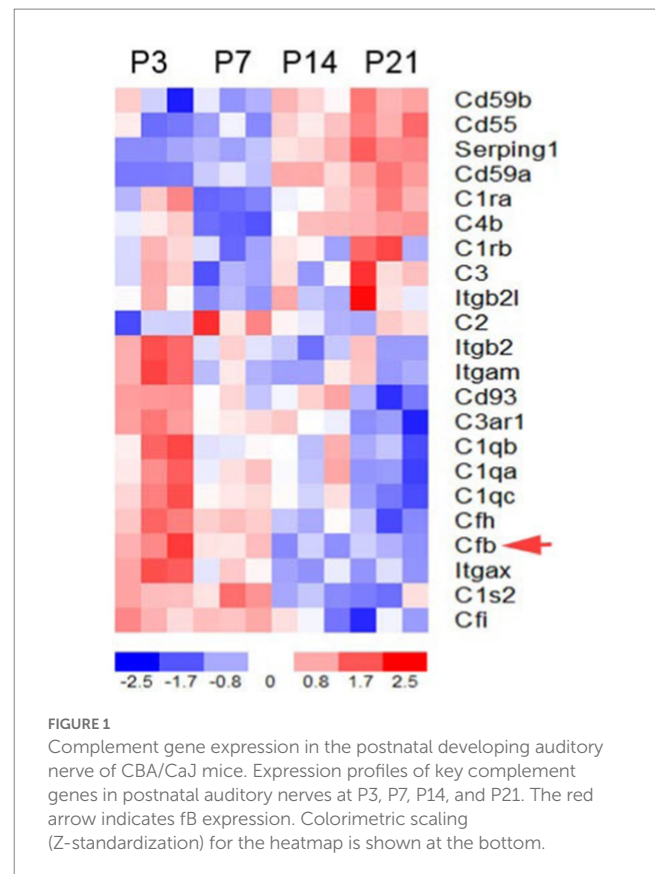
3. Results

3.1. Characterization of complement molecules and factor B in the mouse cochlea

To determine the expression patterns of complement genes in the developing mouse inner ear, we performed RNA sequencing analysis on auditory nerve samples of CBA/CaJ mice aged P3, P7, P14, and P21 (Figure 1). Many key complement genes were differentially expressed in the early postnatal ear (Supplementary Table S1). Clustering analysis of these genes identified two groups of complement-related genes that differed in expression pattern during cochlear development: a group of genes with initially low expression at P0 and a noticeable increase in expression between P7 and P14, and the second group of genes whose expression steadily decreased from P3 to P21, a critical period marked by myelination, hearing onset, and auditory function enhancement. We found fB to be among the cluster with decreasing expression (red arrow).

3.2. Progressive hearing impairment in mice with factor B deficiency

To investigate the impact of fB on auditory function, we utilized a previously generated mouse model of targeted fB deficiency (fB^{-/-} mice) (20, 35). We analyzed auditory brainstem responses (ABR) of wave I thresholds at 1.5 months and 4 months in age-matched WT and fB^{-/-} mice. At 1.5 months, fB^{-/-} mice demonstrated significantly increased ABR thresholds at all frequencies tested compared to the



WT mice (Figure 2A). Additionally, 4-month-old fB^{-/-} mice continued to demonstrate significantly higher ABR thresholds than the WT mice (Figure 2B). ANOVA results using the LMER model of the ABR threshold indicated significant effects of genotype [$F(1,116) = 4.1162$, $p = 0.045$], age [$F(2,670) = 13.052$, $p < 0.001$], and frequency [$F(9,651) = 26.385$, $p < 0.001$], two-way interactions of genotype and age [$F(2,203) = 3.537$, $p = 0.031$], genotype and frequency [$F(9,621) = 4.674$, $p < 0.001$], and age and frequency [$F(18,651) = 7.028$, $p < 0.001$], and a three-way interaction of genotype, age, and frequency [$F(18,651) = 3.702$, $p < 0.001$]. The significant effect of age on the ABR threshold LMER model, indicated a progressive hearing loss in adult fB^{-/-} mice.

ABR supra-threshold function measures revealed decreased wave I amplitudes and delayed wave I latencies at 8, 11.3 and 16 kHz [which represents the apical-middle portion of the cochlea (36); Figures 2C,D]. LMER models of ABR wave I amplitude showed a significant main effect of genotype for the 8 kHz [$F(1,18) = 31.155$, $p < 0.001$], 11.3 kHz [$F(1,11) = 93.786$, $p < 0.001$], and 16 kHz [$F(1,10) = 12.996$, $p = 0.004$] stimulus, in addition to interactions of genotype and stimulus sound pressure level for 8 kHz [$F(10,101) = 3.362$, $p < 0.001$], 11.3 kHz [$F(10,113) = 3.780$, $p < 0.001$] and 16 kHz [$F(7,80) = 5.25$, $p < 0.001$]. Further, LMER models of ABR wave I latency revealed a significant main effect of genotype for the 11.3 kHz [$F(1,20) = 7.127$, $p = 0.015$] tone pips, in addition to interactions of genotype and stimulus sound pressure level for the 8 kHz [$F(10,113) = 2.818$, $p = 0.004$], 11.3 kHz [$F(10,117) = 2.943$, $p = 0.002$], and 16 kHz [$F(8,80) = 3.464$, $p = 0.002$] stimulus. Together these ABR wave I suprathreshold data suggest that pathophysiological

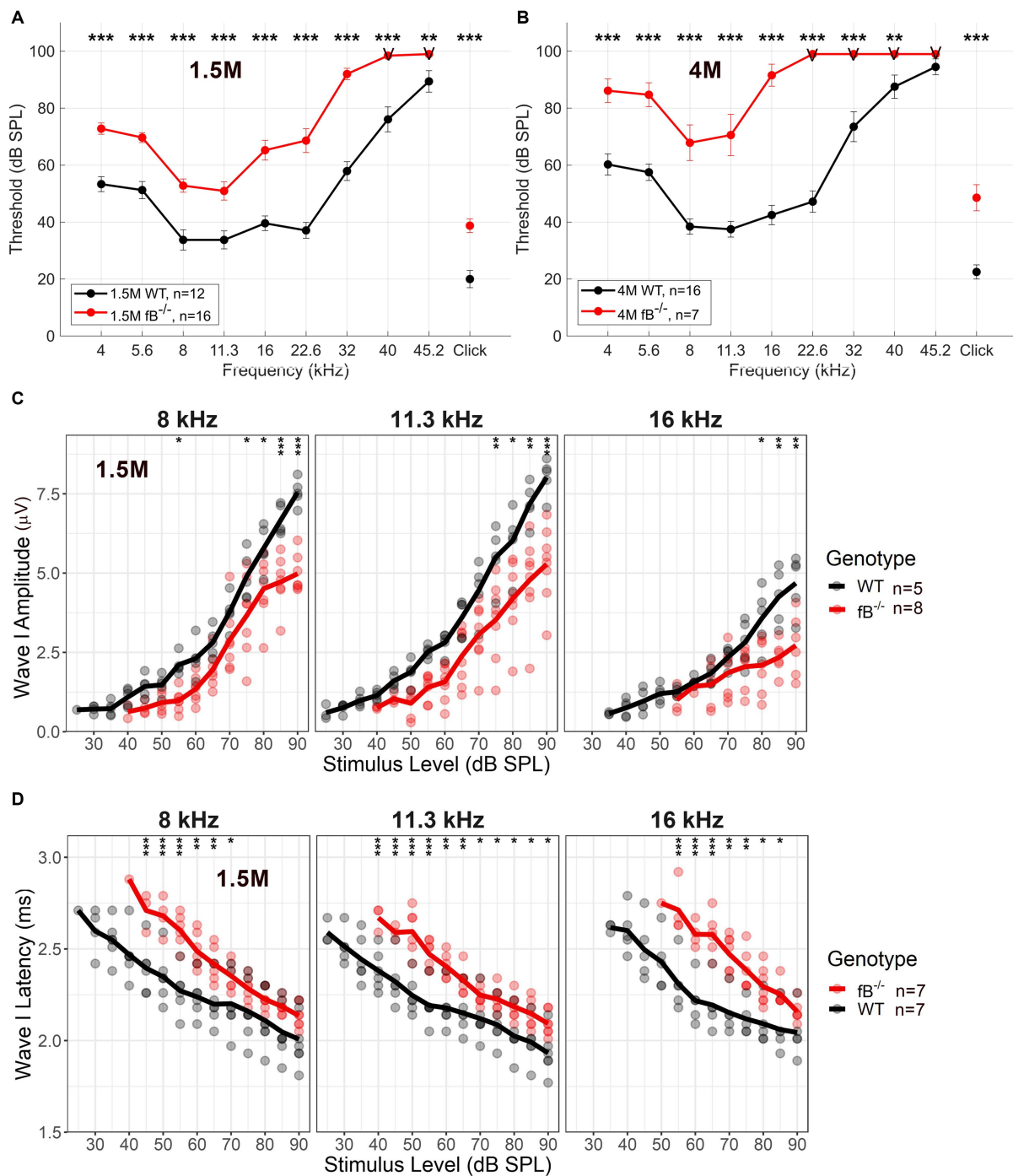


FIGURE 2

Auditory function in fB deficient mice. Auditory Brainstem Response (ABR) was measured in adult WT and fB^{-/-} mice. (A,B) ABR thresholds in 1.5-month (A), and 4-month-old (B) fB^{-/-} mice (red line) and age-matched WT mice (black line). LMER model of the ABR threshold indicated significant effects between WT and fB^{-/-} mice (see Results section). *Post-hoc* pairwise comparisons were conducted to compare genotypes for each frequency at each age, and significant differences between genotypes are denoted in (A,B) with asterisks (* $p < 0.05$, ** $p < 0.01$, *** $p < 0.001$). (C) Average and individual wave I amplitudes for 1.5-month fB^{-/-} and WT mice (randomized subset taken from mice tested in A) in response to 8, 11.3, and 16 kHz stimulus. LMER models of ABR wave I amplitude showed a significant main effect of genotype and stimulus sound pressure level at 8 kHz, 11.3 kHz, and 16 kHz (see Results section). *Post-hoc* pairwise comparisons were conducted to compare amplitudes across genotypes for each sound level, and significant differences between genotypes are denoted with asterisks (* $p < 0.05$, ** $p < 0.01$, *** $p < 0.001$). (D) Average and individual wave I latencies for 1.5-month fB^{-/-} and WT mice (randomized subset taken from mice tested in A) in response to 8, 11.3, and 16 kHz stimulus. LMER models of ABR wave I latency revealed a significant main effect of genotype and stimulus sound pressure level (see Results section) for 8, 11.3, and 16 kHz. *Post-hoc* pairwise comparisons were conducted to compare latencies across genotypes for each sound level, and significant differences between genotypes are denoted with asterisks (* $p < 0.05$, ** $p < 0.01$, *** $p < 0.001$). Error bars in (A,B) represent SEM. "V" in (A,B) indicates that most fB^{-/-} mice showed no response at the examined frequencies.

alterations occur in the peripheral auditory nerve of adult $fB^{-/-}$ mice.

3.3. Gene expression alterations in the auditory nerve of factor B deficient mice

The significant differences in hearing sensitivity and auditory nerve function in $fB^{-/-}$ mice compared to WT mice suggest that pathological changes may have occurred within the auditory nerve of these animals. To further investigate this finding at the molecular level, we performed RNA-sequencing (RNAseq) on the auditory nerves of young adult $fB^{-/-}$ mice to assess gene expression changes that may relate to or contribute to hearing impairment. As shown in Figure 3A, RNAseq analyses identified over 700 genes that were differentially expressed when comparing auditory nerves from adult $fB^{-/-}$ mice to WT mice (p -adjusted <0.05, absolute fold change >1.5; Supplementary Table S2). Analysis of biological processes enriched

among the differentially expressed genes identified processes associated with cell adhesion, extracellular structure organization, neurogenesis, and generation of neurons (Table 1).

Glia cells, including satellite and Schwann cells in the peripheral auditory nerve, are of neural crest origin (37, 38). Interestingly, several genes related to neural crest cell differentiation and myelin function were among those differentially expressed in $fB^{-/-}$ mice (Figures 3B,C). Among these genes, *Notch1*, *Notch2*, *Notch3*, *Trio*, *Cntf*, and *Shank3* are active during neural crest cell migration and differentiation (39–41). *Foxm1* is a gene needed for the renewal of neural progenitor and proliferation of glial cells (42, 43). *Sox4* is a regulator of Schwann cell differentiation (44). Lymphocyte protein (MAL) is an integral membrane protein and plays a role in maintaining myelination (45). Peripheral myelin protein 22 (PMP22) is a key protein that forms the compact myelin of the peripheral nervous system (46). Collectively the differential expression of these genes suggests that *fB* activity is important for the development and function of neural crest cells and myelination in the auditory nerve.

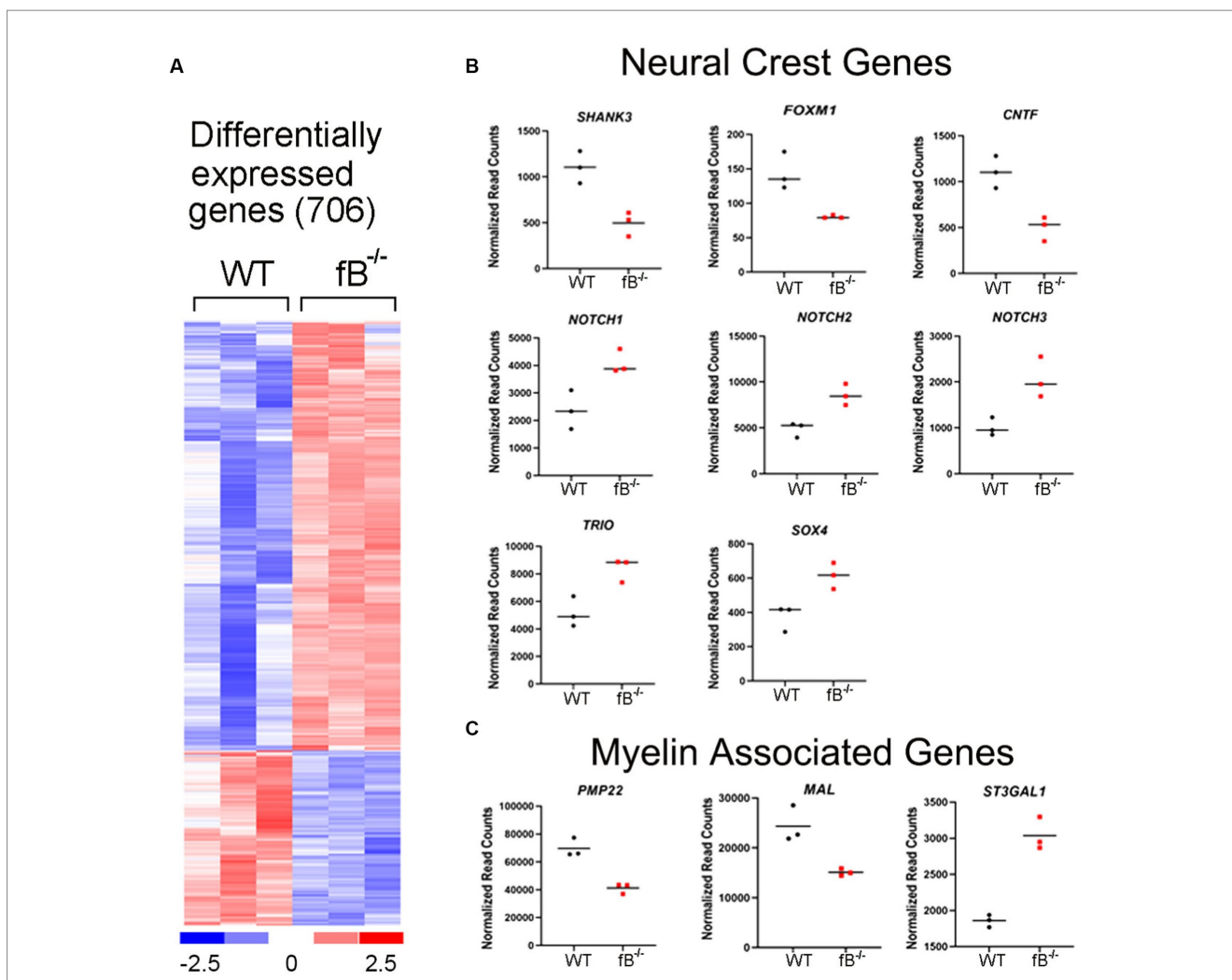


FIGURE 3 Gene expression changes in the auditory nerve of $fB^{-/-}$ mice. (A) Heatmap representation of genes differentially expressed between $fB^{-/-}$ and WT mice. Comparison of auditory nerve tissue from young adult (aged 1.5–2.5 months) $fB^{-/-}$ and WT control animals found that 706 genes were significantly differentially expressed (p -adj <0.05 and absolute fold change >1.5), with 501 being upregulated and 205 being downregulated. (B,C) Read count representation of neural crest genes (*Shank3*, *Foxm1*, *Cntf*, *Notch1*, *Notch 2*, *Notch 3*, *Trio*, and *Sox4*) and myelin-associated genes (*Pmp22*, *Mal*, and *St3gal1*) identified as differentially expressed.

TABLE 1 Gene function enrichment analysis for biological process changes in the auditory nerve of $fb^{-/-}$ mice.

Biological process (top 25 GO names)	<i>q</i> -value Bonferroni
Extracellular structure organization	3.91E-11
External encapsulating structure organization	4.67E-11
Cell adhesion	3.45E-09
Biological adhesion	4.52E-09
Neurogenesis	6.35E-07
Anatomical structure formation involved in morphogenesis	2.26E-06
Cell morphogenesis	3.52E-06
Generation of neurons	8.65E-06
Heart development	1.26E-05
Cellular component morphogenesis	1.32E-05
Cell morphogenesis involved in differentiation	2.96E-05
Cytoskeleton organization	3.07E-05
Supramolecular fiber organization	5.32E-05
Embryo development	9.96E-05
Neuron differentiation	1.10E-04
Circulatory system development	2.14E-04
Behavior	2.36E-04
Cognition	8.85E-04
Central nervous system development	1.03E-03
Sensory organ development	1.20E-03
Cell morphogenesis involved in neuron differentiation	1.31E-03
Embryonic morphogenesis	1.84E-03
Head development	2.19E-03
Neuron projection development	2.25E-03
Regulation of cell differentiation	2.44E-03

3.4. Pathology of glial cells in the auditory nerve of factor B deficient mice

In the auditory nerve of young adult WT mice, type I spiral ganglion neuron (SGN) cell bodies and axons of the auditory nerve were myelinated with satellite cells and Schwann cells, respectively (Figures 4A,A',E). Myelin cell pathologies were present in the auditory nerves of fb knockout mice, including abnormal swirling of myelin sheaths, presence of myelin blebs, and enlarged spaces between satellite cells and the ensheathed SGNs (Figures 4B–D), while satellite cells closely flanked the SGNs in WT auditory nerves. Although the majority of auditory nerve axons showed relatively normal myelination (Figures 4E,F), some Schwann cell abnormalities around the axons were seen, including atypically wide spacing between the Schwann cell cytoplasm and the adjacent axon in $fb^{-/-}$ mice (Figure 4G). Abnormal non-myelinating satellite cells were also present around some of the type II SGNs (Figure 4H). In addition, abnormal development of myelination was seen in the auditory nerve of P14 $fb^{-/-}$ knockout mice (Figure 4J) compared to the aged-matched WT animals (Figure 4I).

To assess the impact of fb deficiency on glial cell function in the auditory nerve, we examined the expression of Na,K-ATPase using an antibody that can identify the $\alpha 1$ isoform of Na,K-ATPase protein. Both $\alpha 1$ and $\alpha 2$ isoforms are expressed in the glial cells of many nervous tissues (47, 48). In particular, Na,K-ATPase $\alpha 1$ was recently reported to express exclusively on satellite glial cells of the human auditory nerve (49). Immunostaining revealed a reduced immunoreactivity of Na,K-ATPase on the satellite glia around SGNs in the auditory nerves of $fb^{-/-}$ mice (Figure 4K), in agreement with pathological alterations of myelin around SGNs identified by EM observation (Figures 4B–D). Together, these results suggest functional declines of auditory nerve activity in $fb^{-/-}$ mice.

To visualize the SGNs, we immunostained auditory nerves with NF200, a marker of sensory neurons. Staining and quantification of SGNs revealed a significant reduction in the number of SGNs in $fb^{-/-}$ mice compared to WT mice in the apical and basal (but not middle) portions of the cochlea (Figures 4L,M) (Mann-Whitney U test; $p=0.03$ for apex; $p=0.47$ for middle; $p=0.04$ for the base). The mean \pm SEM (cells per 10,000 μm^2) of NF200⁺ SGN densities are 29.98 ± 0.7 ($n=4$) and 21.97 ± 2.41 ($n=3$) in the apex, 27.92 ± 2.48 ($n=7$) and 27.15 ± 1.91 ($n=6$) in the middle, and 26.32 ± 1.62 ($n=5$) and 21.13 ± 1.50 ($n=4$) in the base for WT and $fb^{-/-}$ mice, respectively. This suggests that fb deficiency has a negative impact on the SGNs in the apical and basal portions of the cochlea.

Immune cells, such as macrophages, are another key element of the innate immune system, and a major source of complement protein production [see review (50)]. Recent studies have demonstrated that macrophage phenotype is impacted by the presence of complement factors (51–54). We hypothesized that macrophage activity is reactive to changes in complement signaling and therefore, fb deficiency may lead to a reduction of macrophage activity in the auditory nerve. Using ultrastructural analysis, we identified macrophages in several areas of the cochlea in WT and $fb^{-/-}$ mice. In the auditory nerves of the WT mice, it is relatively difficult to identify macrophages. The cellular processes of these macrophage-like cells are often thinner with limited vacuoles (Figures 5A–C). Surprisingly, macrophages in $fb^{-/-}$ mice contained increased lysosomes, abundant rough endoplasmic reticulum, and increased phagoliposomes and vacuoles (24, 25, 28, 55), characteristics that suggest these macrophages were in an activated state. Activated macrophages were seen throughout the auditory nerves of $fb^{-/-}$ mice, particularly in regions around the auditory nerve microvasculature (Figures 5D–F), opposing our original hypothesis. Immunodetection of IBA1, a calcium-binding protein expressed in the cytoplasm of microglia/macrophages, also showed that macrophages were present in the cochlea of fb knockout mice (Figure 5G). Here, we found that macrophages demonstrated a range of morphologies between $fb^{-/-}$ and WT mice, suggesting a diverse range of macrophage functions and phenotypes. In agreement with the EM observations, IBA1⁺ cells were identified with fewer long cellular processes in the auditory nerves of fb knockout mice (Figure 5G), suggesting an activated state of macrophages in $fb^{-/-}$ mice. However, quantitative analysis of IBA1⁺ cells detected no significant differences in the numbers of macrophages between WT and $fb^{-/-}$ mice in most of the cochlear areas, except a reduction was seen in the apical cochlear portion within the osseous spiral lamina (OSL) and the middle cochlear portion within the Rosenthal's canal

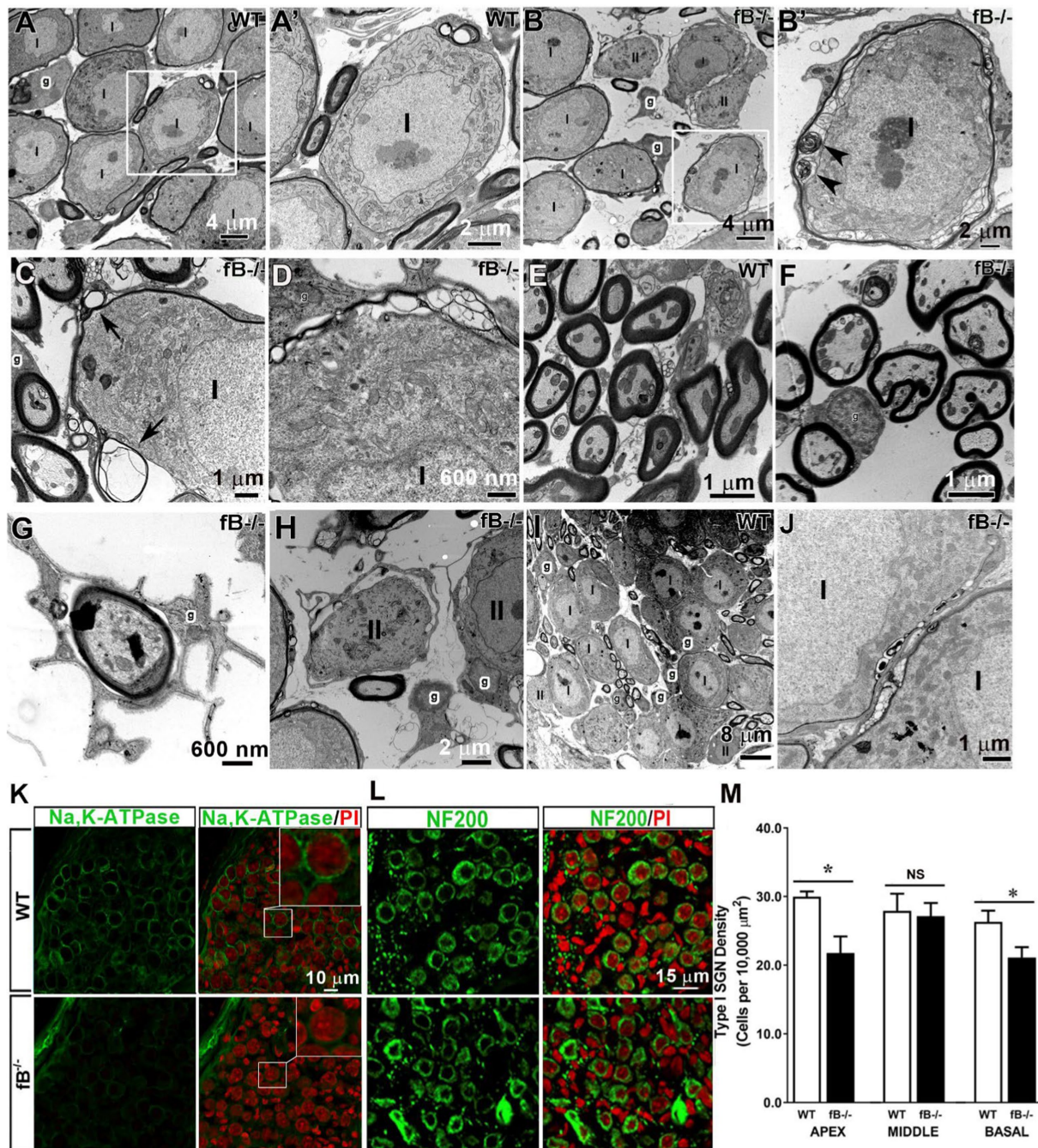


FIGURE 4

Pathophysiological changes of glial cells in the auditory nerve of fb knockout mice. (A–H) Electron micrographs of Rosenthal's canal in adult WT (A,A',C,I) and fb^{-/-} (B,B',D–H,J) mice. (A') is the high magnification of the enclosed areas in the WT (A) auditory nerve revealing tight associations between the myelin of satellite glial cells (g) and type I (I) SGNs. (B) is the high magnification of the enclosed area in (B) showing abnormal swirling of myelin sheaths around type I SGNs (black arrowheads) of fb^{-/-} mice. Similar changes in myelination of SGNs were seen in type I SGNs of the other young adult fb^{-/-} mice (C,D). Arrowheads point out myelin whorls in the myelination surrounding SGNs in (C). (E–G) Electron micrographs of axons in the osseous spiral lamina (OSL) of WT (E) and fb^{-/-} (F,G) mice. The majority of myelinating glial cells around the axon appear relatively normal in the fb knockout mice (F). Enlarged space between the glial cells and the axon of the auditory nerve in an fb^{-/-} mouse (G). (H) Pathological changes were also seen in the non-myelinating glial cells around type II (II) SGNs. (I,J) Similar myelin pathological changes were also seen in the postnatal fb^{-/-} mice (P14) (J), although the development of SGNs shows no abnormalities (I). (K) Confocal images showing Na,K-ATPase immunoreactivity in satellite glial cells surrounding SGNs in young adult WT (the top panel) and fb^{-/-} (bottom panel) mice. Confocal images of both WT and fb^{-/-} mice were obtained using the same microscope acquisition settings. Images in the top-right of the right panel are enlarged images of boxed areas in the center. A reduced Na,K-ATPase immunoreactivity is seen between WT and fb^{-/-} mouse samples. Images were taken from the basal portion of the mouse cochleae. (L,M) Neuron densities are significantly reduced in the apical and basal portions but not in the middle portion in fb^{-/-} mouse cochleae. Confocal images of NF200⁺ neurons in the middle turn of young adult WT (the top panel) and fb^{-/-} (the bottom panel) mice. Propidium iodide (PI) was used to counterstain cell nuclei. Scale bar = 20 μm . Quantification of SGNs in WT and fb^{-/-} mice revealed significant decreases of SGNs in the apical and basal portions of the auditory nerve and no significant loss of SGNs (M). Data bars represent mean density; error bars represent SEM; Data were analyzed by Mann-Whitney U test with statistical significance defined as a *p value of ≤ 0.05 (see detailed information in the Result section).

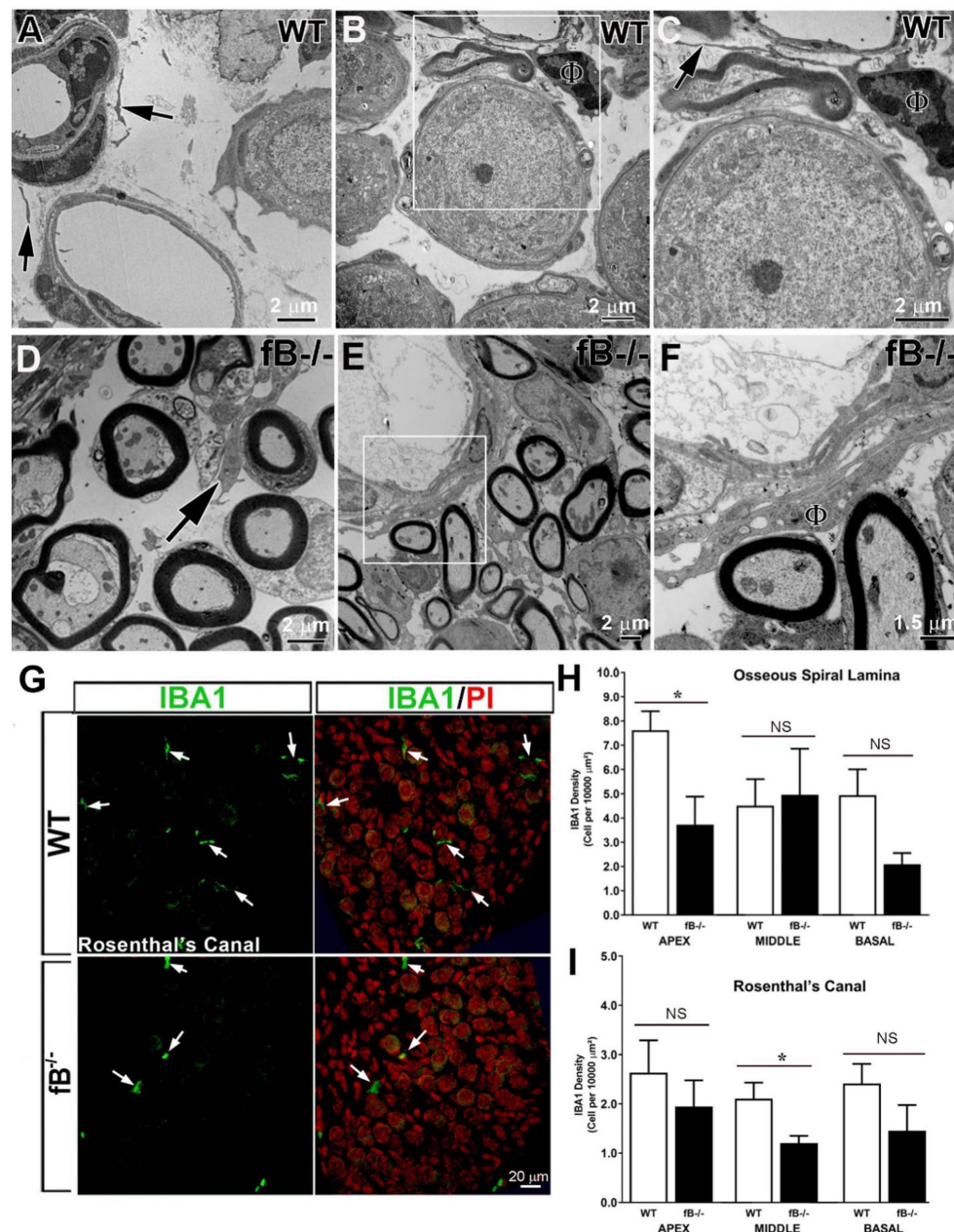


FIGURE 5

Complement fB deficiency does not significantly alter macrophage numbers in the adult auditory nerve. (A–F) Electron micrographs of macrophages (black arrows) in the auditory nerve of young adult WT (A–C), young adult fB^{-/-} (B,C) and P16 fB^{-/-} (B,C) mice. (C) is a magnification of the boxed area in (B) showing a macrophage (ϕ) around a blood vessel with a long and thin cellular process (arrow). An arrow in (D) identifies a macrophage around the axons of the auditory nerve. (F) is a magnification of the boxed area in (E) showing an activated macrophage (ϕ) around a blood vessel. (G) Confocal images of IBA1⁺ macrophages in young adult WT (top panels) and fB^{-/-} (bottom panels) mice. The images were taken within Rosenthal's canal (RC) of the middle portions of the mouse cochleas. Nuclei were counterstained with PI. (H–I) Quantification of IBA1⁺ macrophages revealed no significant changes in macrophage numbers in most cochlear areas except in the apical portion within the osseous spiral lamina (OSL) and middle portion within RC in fB^{-/-} mice. Data bars represent mean; error bars represent SEM. For the auditory nerve in the OSL, $n = 7$ and 6 , $n = 6$ and 5 , and $n = 6$ and 4 cochleas for WT and fB^{-/-} mice in the apex, middle and base, respectively; For the auditory nerve within the RC, $n = 5$ and 4 , $n = 6$ and 5 , and $n = 7$ and 5 cochleas for WT and fB^{-/-} mice in the apex, middle and base, respectively. Analysis was done with the Mann-Whitney U test; statistical significance was defined as a * p value of ≤ 0.05 .

(RC) in the fB^{-/-} mouse auditory nerves (Figures 5H,I) (p values for the auditory nerve in the OSL are 0.021, 0.331, and 0.086 for the apex, middle and base, respectively; p values for the auditory nerve within the RC are 0.278, 0.026, and 0.134 for the apex, middle and

base, respectively). These findings suggest that fB deficiency induces macrophage activation and phenotypic alterations, yet has a limited impact on macrophage numbers in the cochlea highlighting the complex dynamic between macrophages and complement signaling.

3.5. Histopathology of the stria vascularis in factor B deficient mice

Given that perivascular-resident macrophage-like melanocytes reside in the stria vascularis (56) and that strial intermediate cells are also neural crest-derived cells (57), we examined if fB deficiency leads to pathological alterations in the stria vascularis of the cochlear lateral wall. In the stria vascularis of WT mice, the mitochondria-enriched cytoplasmic processes of strial intermediate cells interdigitate tightly with the more electron-dense processes of marginal cells and the fibrous process of the basal cells (Figures 6A–C). However, in fB^{-/-} mice, cells in the stria vascularis appeared to be separated by a larger space, particularly in postnatal animals (Figures 6D–I). Additionally, processes extending from activated macrophages were rarely apparent in the stria vascularis of the WT mice, but these cells were readily detected in the stria vascularis of fB^{-/-} mice (Figure 6E). These macrophage-like cells were identified by special features of activated macrophage including densely packed cytoplasm filled with multiple lysosomes, electron-dense lipid bodies and phagoliposomes as described in our previous studies (24). These strial pathologies and activated macrophages were also seen in postnatal fB^{-/-} mice (Figure 6F). For both young adult and postnatal mice, the well-organized interdigitation among marginal cells, intermediate cells, and basal cells in the stria vascularis was mostly disrupted or lost in fB^{-/-} mice (Figures 6D–I).

Next, we examined the changes of the potassium channel proteins Kir4.1 and Na,K-ATPase in the stria vascularis in fB^{-/-} mice. Kir4.1 and several isoforms of Na,K-ATPase including $\alpha 1$ have been used to evaluate the functional state of the strial intermediate cells and marginal cells, respectively (49, 58–60). Both proteins are essential for generating the endocochlear potential, in the cochlear lateral wall (59, 61, 62). We found that Kir4.1 immunoreactivity was substantially diminished in fB^{-/-} mice (Figure 7A). Kir4.1 immunoreactivity was measured by the fluorescence density of Kir4.1 immunostaining (Mann-Whitney U test; $p = 0.015$ for both the middle and base). There were also additional instances where the integrity of the stria vascularis was compromised, evidenced by gaps in Kir4.1 immunostaining, suggesting a total loss of Kir4.1 immunoreactivity in these strial areas of fB^{-/-} mice (Figure 7A arrows). Focusing on the basal turn of the cochlea, an area where we saw a severe loss of marginal cell-intermediate cell interdigitation, quantitative analysis revealed significantly diminished Kir4.1 immunoreactivity in fB^{-/-} mice (Figure 7B). However, limited changes in Na,K-ATPase immunoreactivity in the marginal cells were seen in the stria vascularis (Supplementary Figure S1). Together with the electron microscopy data shown in Figure 6, these immunostaining data suggest that fB activity plays a role in maintaining the structural and functional integrity of the strial intermediate cells, a neural crest derived cell in the cochlear lateral wall.

3.6. Cochlear hair cells remain in factor B deficient mice

Given the hearing impairment of fB^{-/-} mice, we evaluated organ of Corti structures in both WT and fB^{-/-} mice. Toluidine blue staining of cochlear sections (Figures 8A,B) and ultrastructural examination (Figures 8C–F) revealed that there was minimal pathological

alteration in sensory hair cells of young adult fB^{-/-} mice. To validate this result, we analyzed the immunoreactivity of the hair cell marker Myosin VIIA. We did not find a significant loss in inner or outer hair cells of fB^{-/-} mice (Figures 8G,H). Together, these results suggest that fB deficiency has limited impact on sensory hair cell morphology.

4. Discussion

The complement system is widely expressed in central and peripheral nerves. Complement signaling has been associated with several neurological disorders, including traumatic brain injury, age-related macular degeneration, and Alzheimer's disease (63–68). While most studies focus on the impact of the classical complement pathway, the role of alternative complement signaling in neuronal dysfunction and disorder remains to be explored. Using a well-established mouse model of fB deficiency (20), our study demonstrated that alternative complement signaling is required for the development and maintenance of auditory function. Mice deficient in fB signaling displayed elevated ABR thresholds, decreased ABR wave I amplitudes, and delayed ABR wave I latencies. Additionally, we found that adult fB knockout mice displayed multiple pathologies of the peripheral auditory system, including abnormalities in the auditory nerve and stria vascularis of the cochlear lateral wall. Our study is the first to reveal that proper functioning of the alternative complement pathway is required for the development and maintenance of two key non-sensory cochlear cell types, glial cells, and intermediate cells, which are derived from the neural crest.

The alternative complement pathway acts as a feedback mechanism, via amplifying complement signaling as fB binds to hydrolyzed C3b proteins. Alternative complement signaling has been linked to increased inflammation in the brain after traumatic brain injury (69, 70) and retinal tissue during age-related macular degeneration (71). In addition, fB^{-/-} mice that have undergone cerebral ischemia–reperfusion injury demonstrate reduced neurological pathologies and display protection from demyelination (22). Further, inhibition of the alternative complement pathway, via administration of neutralizing antibodies or genetic deletion, results in decreased neuroinflammation and decreased neurodegeneration in traumatic brain injury and multiple sclerosis (69, 72, 73), suggesting that depleting alternative complement signaling can be protective under pathological conditions. Other studies have shown that fB deletion can be protective and generate positive impacts (74, 75). For example, rats with genetically depleted fB exhibit increased metabolic and cardiovascular function in spontaneous hypertensive rodents. Collectively, these observations suggest that the relationship between fB signaling and disease exacerbation or amelioration may be dependent on disease models and the severity of pathological conditions. However, the effect of fB signaling deficiency in a non-pathological or developmental context is less well-studied. Here we observed that fB deficiency elicited hearing loss at all ages tested, from young adult through old adult stages. Our results support the view that fB signaling is required for normal hearing onset and maintenance of adult auditory function in the non-pathological condition.

Using RNA-seq, we found that several biological processes were significantly impacted by fB deficiency in the auditory nerve, including extracellular structure and organization, neurogenesis, cognition and

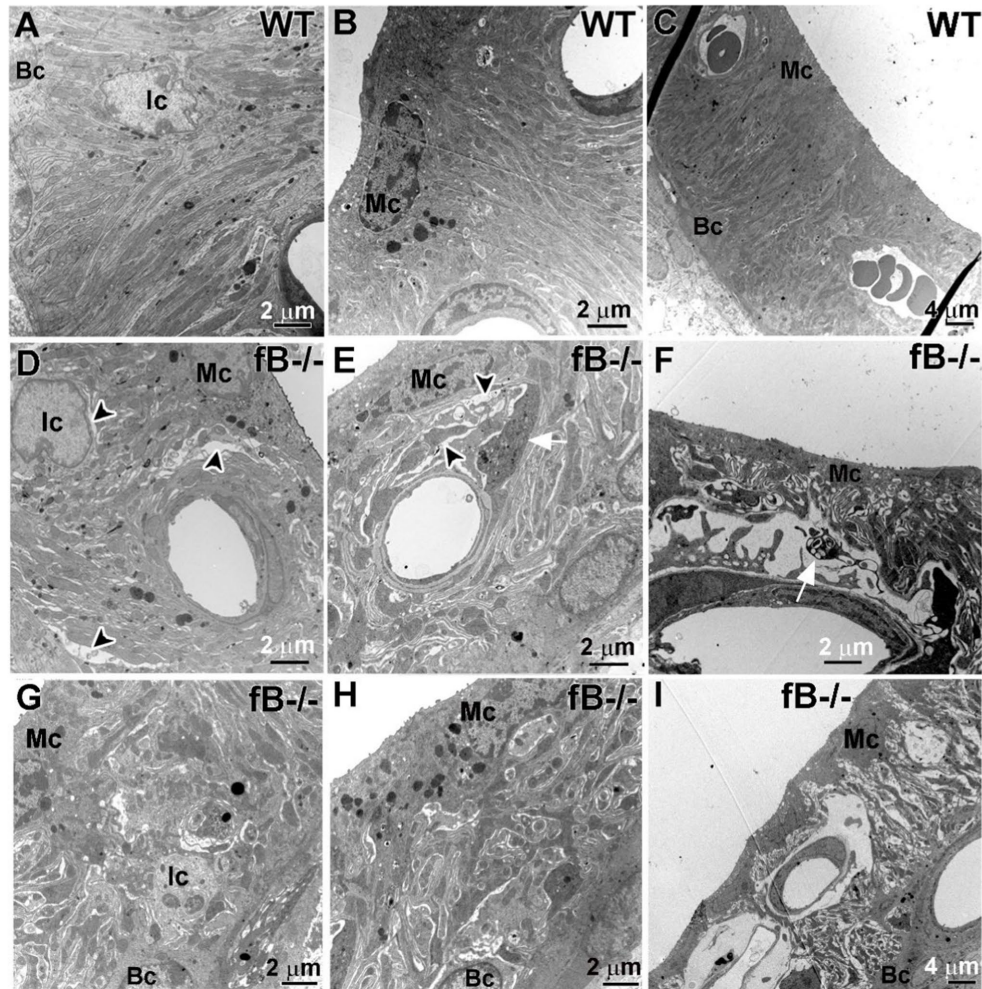


FIGURE 6

fB deficiency results in cochlear stria vascularis pathologies. (A–F) Electron micrographs of the stria vascularis in the cochlear lateral wall of WT (A–C) and fB^{-/-} (D–I) mice. In young adult fB^{-/-} mice (D,E,G,H), the integrity of the interdigitation among intermediate cells (Ic), marginal cells (Mc) and basal cells (Bc) is disrupted or lost (black arrowheads), while their age-matched WT controls have well-organized interdigitation in the stria vascularis (A–C). (F,I) Substantial pathological alterations were seen in the stria vascularis of postnatal fB^{-/-} mice (P16 mouse in F; P14 mouse in I). A white arrow shows macrophage-like processes within the space between the intermediate cells and marginal cells.

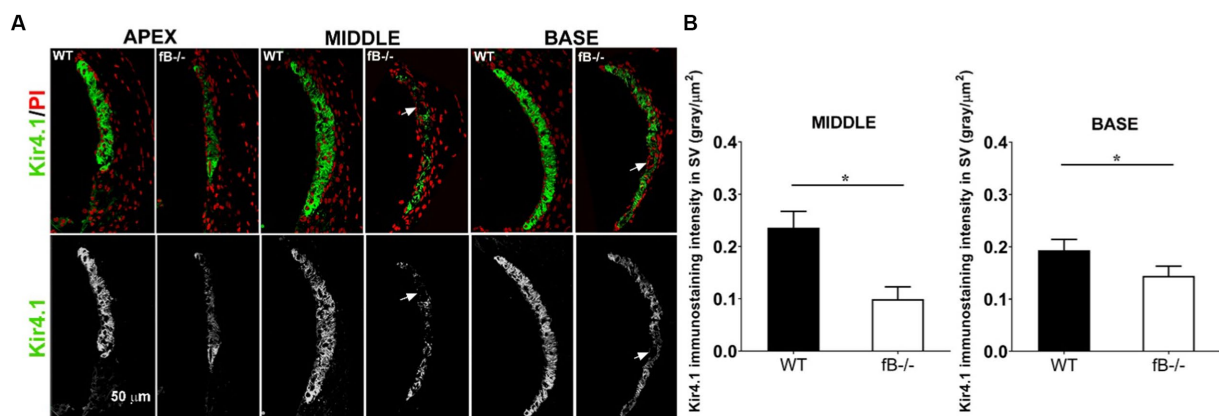


FIGURE 7

Kir4.1 immunoreactivity reduction in fB^{-/-} mice. (A) Confocal representations of Kir4.1 staining in the cochlear lateral wall of WT and fB^{-/-} mice reveal diminished expression in fB^{-/-} mouse cochleae. Propidium iodide (PI) was used to counterstain cell nuclei. (B) A significantly reduced Kir4.1 immunoreactivity was seen in the middle and basal stria vascularis of the fB^{-/-} mice. Data bars represent the mean; error bars represent SEM. $n = 6$ and 5 cochleas for the middle turn in WT and fB^{-/-} group, respectively; $n = 7$ and 5 cochleas for the basal turn WT and fB^{-/-} group, respectively. Analysis was done with the Mann-Whitney U test; statistical significance was defined as a * p value of ≤ 0.05 .

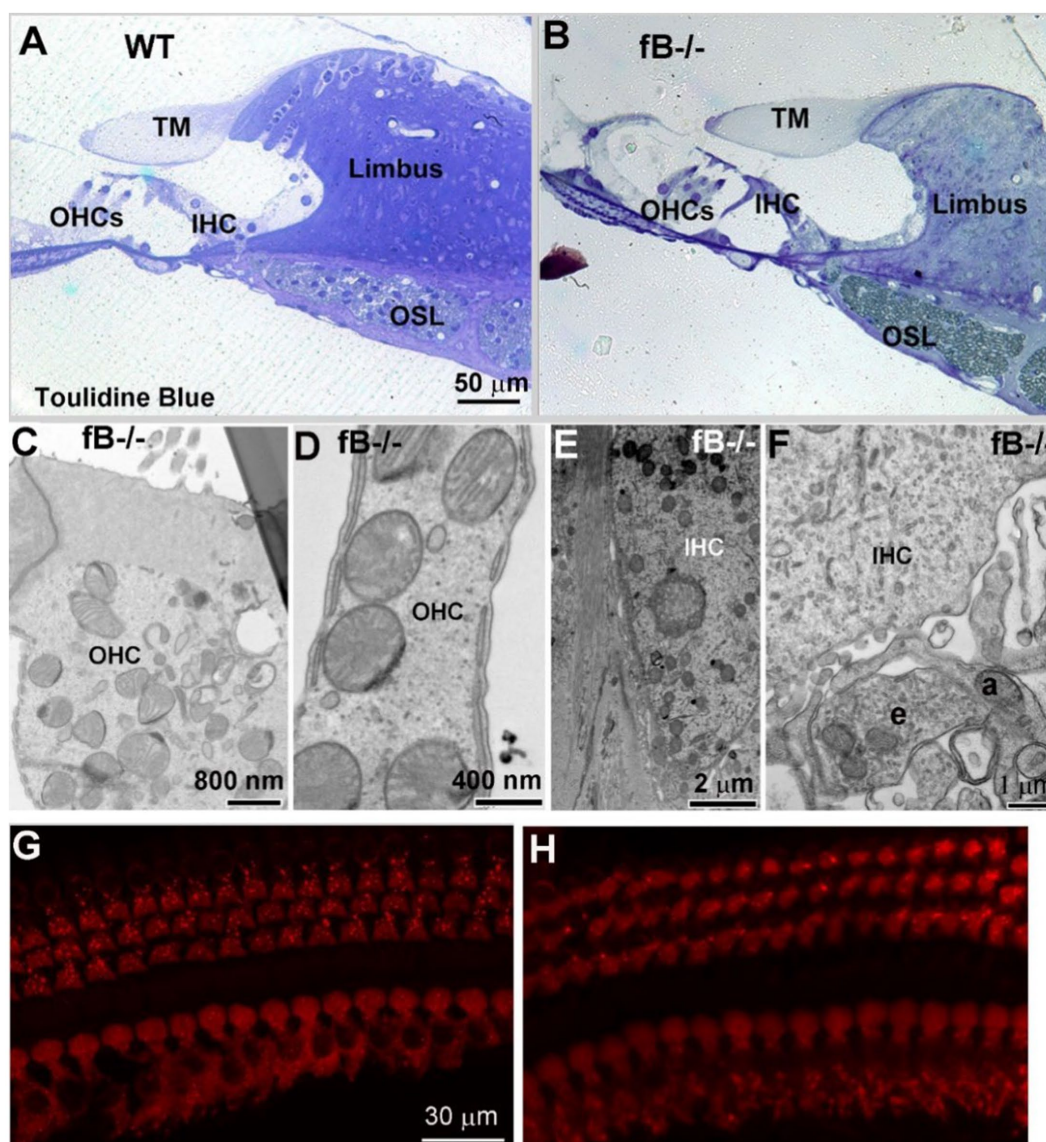


FIGURE 8

The organ of Corti histology is comparable in $fB^{-/-}$ and WT mice. (A,B) Light microscopy of toluidine blue-stained 1-month WT and $fB^{-/-}$ cochlear samples. Representative images of the organ of Corti of WT (A) and $fB^{-/-}$ (B) mice. TM, tectorial membrane; OSL, osseous spiral lamina; OHC, outer hair cell; IHC, inner hair cell. Images in (A,B) were representative images taken from the middle portion of mouse cochleas. Two mice per group were observed. (C–F) Normal ultra-structures of OHCs and IHCs in young adult $fB^{-/-}$ cochleas. An efferent (e) terminal connects with an afferent terminal (a) underneath of an inner hair cell. (G,H) Confocal microscopy of Myosin VIIa⁺ hair cells in WT (G) and $fB^{-/-}$ (H) cochleas. Hair cells are well preserved in both mouse strains.

behavior, central nervous system development, and generation of neurons. When analyzing differentially expressed genes in fB knockout mice, we found several genes that were associated with neural crest cell development and myelination. Interestingly, we observed a significant loss in the number of spiral ganglion neurons in fB knockout compared to control mice in both the apical and basal portions of the cochleas. We also found obvious pathologies in the myelin sheath of the auditory nerve and abnormalities in the stria vascularis of the cochlear lateral wall. Recent studies found that complement genes contribute to neural crest cell migration during embryonic development (76, 77). Given that auditory glia and cochlear melanocytes (such as intermediate cells of the stria vascularis)

are derived from neural crest cells (28, 49, 78), fB may be important for neural crest cell function. Further, glial cell-specific pathologies may be the underlying cause for delayed ABR wave I latencies seen in $fB^{-/-}$ mice (Figure 2). Additionally, auditory glial cells support, nourish, protect, and influence the function of spiral ganglion neurons (79–81). Given the important supportive role that glial cells exert on neighboring neurons, the presence of pathology among glial cells in the auditory nerve in $fB^{-/-}$ mice could be the causative factor of the decreased spiral ganglion neuron numbers we identified in these fB knockout mice.

Our results also revealed the indirect influence of fB signaling on the maintenance of cochlear ion homeostasis. When analyzing

Kir4.1 in the cochlear lateral wall of $fB^{-/-}$ mice, we found that expression of this protein was significantly reduced, when compared to WT mice. Kir4.1 is critical for the rectifying of K^+ by intermediate cells in the cochlear lateral wall for proper generation and maintenance of the endocochlear potential (82, 83). Also, Kir4.1 channels on the surface of glial cells play a critical role in siphoning extracellular K^+ released by neurons during activity (84, 85). Mice lacking Kir4.1 signaling demonstrate profound hearing loss due to a reduced endocochlear potential, and a diminished ability of glial cells to expel SGN-released K^+ ions (82, 85). Although not investigated in this study, future studies should focus on determining if the pathological alterations that we identified in the stria vascularis of the cochlear lateral wall results in reduced endocochlear potential in $fB^{-/-}$ mice.

Since there were no apparent pathologies in the structures of the organ of Corti, including the inner and outer hair cells, it is likely auditory dysfunction in $fB^{-/-}$ mice is largely due to the pathologies in the auditory nerve and cochlear lateral wall. Although we did not examine hair cell functional alterations in this study (e.g., changes in distortion product otoacoustic emissions), our data revealed increased ABR thresholds and impaired suprathreshold functioning, indicating dysfunction of the peripheral auditory nerve in young adult mice. A previous study found limited cochlear pathological alterations in animal models deficient in the classical complement molecule *C1qa* (86). Hair cell specific complement *C1q like 1* (*C1ql1*) deletion leads to no changes in hearing sensitivity (15), however, a significant hearing loss together with auditory nerve pathology has been reported in the global *C1ql1* deficiency model (16). The alternative complement pathway is responsible for ~80% of complement activity (87). Thus, our finding of hearing impairment in $fB^{-/-}$ mice highlights the importance of comprehensive investigation into alternative complement signaling. Further studies should be aimed at exploring (1) molecular regulation of alternative complement signaling in the development and function of neural crest derived cells in the cochlea, and (2) if alternative complement signaling contributes to hair cell innervation and the maturation of pre- and postsynaptic connections in the auditory nerve.

Additionally, deficiency in fB has been linked to the suppression of immune responses. For instance, previous literature has shown that mice deficient in both fB and $C2$ of the alternative pathway were at a higher risk of contracting renal fungal infections (74, 88). These mice also demonstrated a delayed opsonophagocytic effect and subsequently displayed higher levels of infection in the kidneys (88). Also, fB knockout mice displayed lower airway responsiveness to the toxic agent methacholine and demonstrated remarkably less airway inflammation (89).

Interestingly, we found limited changes in the macrophage numbers between $fB^{-/-}$ and WT mice. However, we did find macrophages in activated states in fB -deficient mice, although we did not further investigate phenotypic changes in cochlear macrophages. Studies show that macrophages respond to molecular signaling changes in their microenvironment (90–92). Considering the regulatory role that complement signaling exerts on macrophages, and the previously established role of cochlear macrophages in auditory nerve development (24, 93, 94), cochlear injury repair (95–98), and stria vascularis function, (56, 99, 100), future studies should be aimed at examining potential macrophage-specific alterations

related to complement signaling, such as the regulation of pro-inflammatory and anti-inflammatory macrophage activation states. Additionally, given the important role that macrophages play in the inflammaging of the mouse cochlea (4, 101), it will be important to further investigate the pathological alterations in aged $fB^{-/-}$ mice.

Here we report the important role of the complement pathway in hearing function and the preservation of the cochlear structure. We found that complement proteins, including factors related to the alternative signaling pathway, are expressed in the developing and adult mouse cochlea. Mice deficient in fB signaling exhibited progressive hearing impairment, however, these animals do not appear to have robust hair cell abnormalities. While SGNs in the auditory nerves of $fB^{-/-}$ mice appeared unaltered, severe pathology was discovered in the ultrastructure of satellite/Schwann cells in the auditory nerve, and abnormal architecture in the stria vascularis of the cochlear lateral wall was identified. Collectively, these results indicate that alternative complement signaling is important for peripheral auditory system function. Additional studies should elucidate the source of complement signaling in the cochlea and the mechanism by which the alternative complement pathway exerts its influence.

Data availability statement

The datasets presented in this study can be found in online repositories. The names of the repository/repositories and accession number(s) can be found in the article/[Supplementary material](#).

Ethics statement

The animal study was reviewed and approved by the Institutional Animal Care and Use Committee of MUSC.

Author contributions

LB, JB, CA, and HL contributed to the conception and design of the study. LB, SJ, and HL performed the research. LB, JB, SJ, JR, TJ, and HL analyzed the data. CA provided the animal model used in the study. LB and HL wrote the manuscript. All authors contributed to the article and approved the submitted version.

Funding

This work was supported by National Institutes of Health Grants F31DC014435 (LB), T32DC014435 (LB, TJ, JR), K18 DC018517 (HL), R56DC012058-06 (HL), R01DC012058 (HL), P50DC000422 (HL), SFARI Pilot Award #649452 (HL), P30GM103342 (JB), P20GM103499 (JB), UL1 TR00145, P30 CA138313, and S10 OD018113 from Cell and Molecular Imaging Shared Resource and Hollings Cancer Center, C06 RR014516 from the Extramural Research Facilities Program of the National Center for Research Resources, and the Medical University of South Carolina Office of the Vice President for Research.

Acknowledgments

We thank Juhong Zhu and Nancy Smythe for their excellent technical assistance. We also thank Jayne Ahlstrom, and Nathaniel Parsons for their comments and editing of the manuscript. Additionally, we thank the Department of Biology at Winthrop University and the Division of Science and Technology at Clinton College for administrative support.

Conflict of interest

The authors declare that the research was conducted in the absence of any commercial or financial relationships that could be construed as a potential conflict of interest.

References

- World Health Organization. Deafness and Hearing. (2023). Available at: <https://www.who.int/news-room/fact-sheets/detail/deafness-and-hearing-loss>.
- Leszek J, Barreto GE, Gasiorowski K, Koutsouraki E, Avila-Rodriguez M, Aliev G. Inflammatory mechanisms and oxidative stress as key factors responsible for progression of neurodegeneration: role of brain innate immune system. *CNS Neurol Disord Drug Targets*. (2016) 15:329–36. doi: 10.2174/1871527315666160202125914
- Watson N, Ding B, Zhu X, Frisina RD. Chronic inflammation - inflammaging - in the ageing cochlea: a novel target for future presbycusis therapy. *Ageing Res Rev*. (2017) 40:142–8. doi: 10.1016/j.arr.2017.10.002
- Noble K, Brown L, Elvis P, Lang H. Cochlear immune response in Presbycusis: a focus on dysregulation of macrophage activity. *J Assoc Res Otolaryngol*. (2021) 23:1–16. doi: 10.1007/s10162-021-00819-x
- Propson NE, Gedam M, Zheng H. Complement in neurologic disease. *Annu Rev Pathol*. (2021) 16:277–98. doi: 10.1146/annurev-pathol-031620-113409
- Stevens B, Allen NJ, Vazquez LE, Howell GR, Christopherson KS, Nouri N, et al. The classical complement cascade mediates CNS synapse elimination. *Cells*. (2007) 131:1164–78. doi: 10.1016/j.cell.2007.10.036
- Schafer DP, Lehrman EK, Kautzman AG, Koyama R, Mardinly AR, Yamasaki R, et al. Microglia sculpt postnatal neural circuits in an activity and complement-dependent manner. *Neuron*. (2012) 74:691–705. doi: 10.1016/j.neuron.2012.03.026
- Lim TK, Ruthazer ES. Microglial trogocytosis and the complement system regulate axonal pruning *in vivo*. *elife*. (2021) 10:e62167. doi: 10.7554/eLife.62167
- Propson NE, Roy ER, Litvinchuk A, Köhl J, Zheng H. Endothelial C3a receptor mediates vascular inflammation and blood-brain barrier permeability during aging. *J Clin Invest*. (2021) 131:e140966. doi: 10.1172/JCI140966
- Bourel J, Planche V, Dubourdieu N, Oliveira A, Sere A, Ducourneau EG, et al. Complement C3 mediates early hippocampal neurodegeneration and memory impairment in experimental multiple sclerosis. *Neurobiol Dis*. (2021) 160:105533. doi: 10.1016/j.nbd.2021.105533
- Hernandez-Encinas E, Aguilar-Morante D, Morales-Garcia JA, Gine E, Sanz-SanCristobal M, Santos A, et al. Complement component 3 (C3) expression in the hippocampus after excitotoxic injury: role of C/EBPbeta. *J Neuroinflammation*. (2016) 13:276. doi: 10.1186/s12974-016-0742-0
- Litvinchuk A, Wan YW, Swartzlander DB, Chen F, Cole A, Propson NE, et al. Complement C3aR inactivation attenuates tau pathology and reverses an immune network deregulated in Tauopathy models and Alzheimer's disease. *Neuron*. (2018) 100:1337–1353.e5. doi: 10.1016/j.neuron.2018.10.031
- Sarma JV, Ward PA. The complement system. *Cell Tissue Res*. (2011) 343:227–35. doi: 10.1007/s00441-010-1034-0
- Merle NS, Church SE, Fremeaux-Bacchi V, Roumenina LT. Complement system part I - molecular mechanisms of activation and regulation. *Front Immunol*. (2015) 6:262. doi: 10.3389/fimmu.2015.00262
- Biswas J, Pijewski RS, Makol R, Miramontes TG, Thompson BL, Kresic LC, et al. C1qI1 is expressed in adult outer hair cells of the cochlea in a tonotopic gradient. *PLoS One*. (2021) 16:e0251412. doi: 10.1371/journal.pone.0251412
- Qi Y, Xiong W, Yu S, Du Z, Qu T, He L, et al. Deletion of C1qI1 causes hearing loss and abnormal auditory nerve fibers in the mouse cochlea. *Front Cell Neurosci*. (2021) 15:713651. doi: 10.3389/fncel.2021.713651
- Patel M, Hu Z, Bard J, Jamison J, Cai Q, Hu BH. Transcriptome characterization by RNA-Seq reveals the involvement of the complement components in noise-

Publisher's note

All claims expressed in this article are solely those of the authors and do not necessarily represent those of their affiliated organizations, or those of the publisher, the editors and the reviewers. Any product that may be evaluated in this article, or claim that may be made by its manufacturer, is not guaranteed or endorsed by the publisher.

Supplementary material

The Supplementary material for this article can be found online at: <https://www.frontiersin.org/articles/10.3389/fneur.2023.1214408/full#supplementary-material>

- traumatized rat cochlea. *Neuroscience*. (2013) 248:1–16. doi: 10.1016/j.neuroscience.2013.05.038
- Ricklin D, Hajishengallis G, Yang K, Lambris JD. Complement: a key system for immune surveillance and homeostasis. *Nat Immunol*. (2010) 11:785–97. doi: 10.1038/ni.1923
- Li Q, Li YX, Stahl GL, Thurman JM, He Y, Tong HH. Essential role of factor B of the alternative complement pathway in complement activation and opsonophagocytosis during acute pneumococcal otitis media in mice. *Infect Immun*. (2011) 79:2578–85. doi: 10.1128/IAI.00168-11
- Matsumoto M, Fukuda W, Circolo A, Goellner J, Strauss-Schoenberger J, Wang X, et al. Abrogation of the alternative complement pathway by targeted deletion of murine factor B. *Proc Natl Acad Sci U S A*. (1997) 94:8720–5. doi: 10.1073/pnas.94.16.8720
- Davis KS, Casey SE, Mulligan JK, Mulligan RM, Schlosser RJ, Atkinson C. Murine complement deficiency ameliorates acute cigarette smoke-induced nasal damage. *Otolaryngol Head Neck Surg*. (2010) 143:152–8. doi: 10.1016/j.otohns.2010.02.022
- Elvington A, Atkinson C, Zhu H, Yu J, Takahashi K, Stahl GL, et al. The alternative complement pathway propagates inflammation and injury in murine ischemic stroke. *J Immunol*. (2012) 189:4640–7. doi: 10.4049/jimmunol.1201904
- Johnson KR, Erway LC, Cook SA, Willott JF, Zheng QY. A major gene affecting age-related hearing loss in C57BL/6J mice. *Hear Res*. (1997) 114:83–92. doi: 10.1016/S0378-5955(97)00155-X
- Brown LN, Xing Y, Noble KV, Barth JL, Panganiban CH, Smythe NM, et al. Macrophage-mediated glial cell elimination in the postnatal mouse cochlea. *Front Mol Neurosci*. (2017) 10:407. doi: 10.3389/fnmol.2017.00407
- Panganiban CH, Barth JL, Darbelli L, Xing Y, Zhang J, Li H, et al. Noise-induced dysregulation of quaking RNA binding proteins contributes to auditory nerve demyelination and hearing loss. *J Neurosci*. (2018) 38:2551–68. doi: 10.1523/JNEUROSCI.2487-17.2018
- Lang H, Li M, Kilpatrick LA, Zhu J, Samuvel DJ, Krug EL, et al. Sox2 up-regulation and glial cell proliferation following degeneration of spiral ganglion neurons in the adult mouse inner ear. *J Assoc Res Otolaryngol*. (2011) 12:151–71. doi: 10.1007/s10162-010-0244-1
- Ruben RJ. The developing concept of Tonotopic Organization of the Inner ear. *J Assoc Res Otolaryngol*. (2020) 21:1–20. doi: 10.1007/s10162-019-00741-3
- Steel KP, Barkway C. Another role for melanocytes: their importance for normal stria vascularis development in the mammalian inner ear. *Development*. (1989) 107:453–63. doi: 10.1242/dev.107.3.453
- Hirose K, Liberman MC. Lateral Wall histopathology and Endocochlear potential in the noise-damaged mouse cochlea. *J Assoc Res Otolaryngol*. (2003) 4:339–52. doi: 10.1007/s10162-002-3036-4
- Love MI, Huber W, Anders S. Moderated estimation of fold change and dispersion for RNA-seq data with DESeq2. *Genome Biol*. (2014) 15:550. doi: 10.1186/s13059-014-0550-8
- Chen JBE, Aronow BJ, Jegga AG. ToppGene suite for gene list enrichment analysis and candidate gene prioritization. *Nucleic Acids Res*. (2009) 37:W305–11. doi: 10.1093/nar/gkp427
- Bates D, Mächler M, Bolker B, Walker S. Fitting linear mixed-effects models using lme4. *J Stat Softw*. (2015) 67:1–48. doi: 10.18637/jss.v067.i01
- Fox J, Weisberg S. *An R companion to applied regression*. 3rd ed. Thousand Oaks CA: Sage (2019).

34. Lenth RV. *Emmeans: Estimated marginal means, aka least-squares means.* (2021).
35. Pekna M, Hietala MA, Landin A, Nilsson AK, Lagerberg C, Betsholtz C, et al. Mice deficient for the complement factor B develop and reproduce normally. *Scand J Immunol.* (1998) 47:375–80. doi: 10.1046/j.1365-3083.1998.00313.x
36. Müller M, von Hünerbein K, Hoidis S, Smolders JW. A physiological place-frequency map of the cochlea in the CBA/J mouse. *Hear. Res.* (2005) 202:63–73.
37. Jessen KR, Mirsky R. Signals that determine Schwann cell identity. *J Anat.* (2002) 200:367–76. doi: 10.1046/j.1469-7580.2002.00046.x
38. Woodhoo A, Sommer L. Development of the Schwann cell lineage: from the neural crest to the myelinated nerve. *Glia.* (2008) 56:1481–90. doi: 10.1002/glia.20723
39. High FA, Zhang M, Proweller A, Tu L, Parmacek MS, Pear WS, et al. An essential role for notch in neural crest during cardiovascular development and smooth muscle differentiation. *J Clin Invest.* (2007) 117:353–63. doi: 10.1172/JCI30070
40. Chalazontis A, Rothman TP, Chen J, Vinson EN, MacLennan AJ, Gershon MD. Promotion of the development of enteric neurons and glia by neurotrophic cytokines: interactions with neurotrophin-3. *Dev Biol.* (1998) 198:343–65. doi: 10.1016/S0012-1606(98)80010-9
41. Si ZP, Wang G, Han SS, Jin Y, Hu YX, He MY, et al. CNTF and Nrf2 are coordinately involved in regulating self-renewal and differentiation of neural stem cell during embryonic development. *iScience.* (2019) 19:303–15. doi: 10.1016/j.isci.2019.07.038
42. Zhang S, Teng H, Ding Q, Fan J, Shi W, Zhou Y, et al. FoxM1 involvement in astrocyte proliferation after spinal cord injury in rats. *J Mol Neurosci.* (2013) 51:170–9. doi: 10.1007/s12031-013-9972-0
43. Besharat ZM, Abballe L, Cicconardi F, Bhutkar A, Grassi L, Le Pera L, et al. Foxm1 controls a pro-stemness microRNA network in neural stem cells. *Sci Rep.* (2018) 8:3523. doi: 10.1038/s41598-018-21876-y
44. Bartesaghi L, Arnaud Gouttenoire E, Prunotto A, Médard J-J, Bergmann S, Christ R. Sox4 participates in the modulation of Schwann cell myelination. *Eur J Neurosci.* (2015) 42:1788–96. doi: 10.1111/ejn.12929
45. Lara-Lemus R. On the role of myelin and lymphocyte protein (MAL) in cancer: a puzzle with two faces. *J Cancer.* (2019) 10:2312–8. doi: 10.7150/jca.30376
46. Li J, Parker B, Martyn C, Natarajan C, Guo J. The PMP22 gene and its related diseases. *Mol Neurobiol.* (2013) 47:673–98. doi: 10.1007/s12035-012-8370-x
47. McGrail KM, Phillips JM, Sweadner KJ. Immunofluorescent localization of three Na,K-ATPase isozymes in the rat central nervous system: both neurons and glia can express more than one Na,K-ATPase. *K-ATPase J Neurosci.* (1991) 11:381–91. doi: 10.1523/JNEUROSCI.11-02-00381.1991
48. Kinoshita PF, Yshii LM, Orellana AMM, Paixão AG, Vasconcelos AR, Lima LS, et al. Alpha 2 Na+,K+-ATPase silencing induces loss of inflammatory response and ouabain protection in glial cells. *Sci Rep.* (2017) 7:4894. doi: 10.1038/s41598-017-05075-9
49. Liu T, Li G, Noble KV, Li Y, Barth JL, Schulte BA, et al. Age-dependent alterations of Kir4.1 expression in neural crest-derived cells of the mouse and human cochlea. *Neurobiol Aging.* (2019) 80:210–22. doi: 10.1016/j.neurobiolaging.2019.04.009
50. Pollard JW. Trophic macrophages in development and disease. *Nat Rev Immunol.* (2009) 9:259–70. doi: 10.1038/nri2528
51. Fraser DA, Arora M, Bohlsón SS, Lozano E, Tenner AJ. Generation of inhibitory NfκB complexes and phosphorylated cAMP response element-binding protein correlates with the anti-inflammatory activity of complement protein C1q in human monocytes. *J Biol Chem.* (2007) 282:7360–7. doi: 10.1074/jbc.M605741200
52. Asgari E, Le Fric G, Yamamoto H, Perucha E, Sacks SS, Kohl J, et al. C3a modulates IL-1β secretion in human monocytes by regulating ATP efflux and subsequent NLRP3 inflammasome activation. *Blood.* (2013) 122:3473–81. doi: 10.1182/blood-2013-05-502229
53. Gavin C, Meinke S, Heldring N, Heck KA, Achour A, Iacobaeus E, et al. The complement system is essential for the phagocytosis of mesenchymal stromal cells by monocytes. *Front Immunol.* (2019) 10:2249. doi: 10.3389/fimmu.2019.02249
54. Bohlsón SS, O'Conner SD, Hulsebus HJ, Ho MM, Fraser DA. Complement, c1q, and c1q-related molecules regulate macrophage polarization. *Front Immunol.* (2014) 5:402. doi: 10.3389/fimmu.2014.00402
55. Liu W, Molnar M, Garnham C, Benav H, Rask-Andersen H. Macrophages in the human cochlea: saviors or predators—a study using super-resolution immunohistochemistry. *Front Immunol.* (2018) 9:223. doi: 10.3389/fimmu.2018.00223
56. Zhang W, Dai M, Fridberger A, Hassan A, Degagne J, Neng L, et al. Perivascular-resident macrophage-like melanocytes in the inner ear are essential for the integrity of the intrastrial fluid-blood barrier. *Proc Natl Acad Sci U S A.* (2012) 109:10388–93. doi: 10.1073/pnas.1205210109
57. Hilding DA, Ginzberg RD. Pigmentation of the stria vascularis. The contribution of neural crest melanocytes. *Acta Otolaryngol.* (1977) 84:24–37. doi: 10.3109/00016487709123939
58. Schulte BA, Adams JC. Distribution of immunoreactive Na+,K+-ATPase in gerbil cochlea. *J Histochem Cytochem.* (1989) 37:127–34. doi: 10.1177/37.2.2536055
59. Chen J, Zhao HB. The role of an inwardly rectifying K(+) channel (Kir4.1) in the inner ear and hearing loss. *Neuroscience.* (2014) 265:137–46. doi: 10.1016/j.neuroscience.2014.01.036
60. Korrapati S, Taukulis I, Olszewski R, Pyle M, Gu S, Singh R, et al. Single cell and single nucleus RNA-Seq reveal cellular heterogeneity and homeostatic regulatory networks in adult mouse Stria Vascularis. *Front Mol Neurosci.* (2019) 12:316. doi: 10.3389/fnmol.2019.00316
61. Marcus DC, Wu T, Wangemann P, Kofuji P, KCN10 (Kir4.1) potassium channel knockout abolishes endocochlear potential. *Am J Physiol Cell Physiol.* (2002) 282:C403–7. doi: 10.1152/ajpcell.00312.2001
62. Wangemann P, Itza EM, Albrecht B, Wu T, Jabba SV, Maganti RJ, et al. Loss of KCN10 protein expression abolishes endocochlear potential and causes deafness in Pendred syndrome mouse model. *BMC Med.* (2004) 2:30. doi: 10.1186/1741-7015-2-30
63. Kossman T, Stahel PF, Morganti-Kossmann MC, Jones JL, Barnum SR. Elevated levels of the complement components C3 and factor B in ventricular cerebrospinal fluid of patients with traumatic brain injury. *J Neuroimmunol.* (1997) 73:63–9. doi: 10.1016/S0165-5728(96)00164-6
64. Ingram G, Loveless S, Howell OW, Hakobyan S, Dancy B, Harris CL, et al. Complement activation in multiple sclerosis plaques: an immunohistochemical analysis. *Acta Neuropathol Commun.* (2014) 2:53. doi: 10.1186/2051-5960-2-53
65. Wu T, Dejanovic B, Gandham VD, Gogineni A, Edmonds R, Schauer S, et al. Complement C3 is activated in human AD brain and is required for neurodegeneration in mouse models of amyloidosis and Tauopathy. *Cell Rep.* (2019) 28:2111–2123.e6. doi: 10.1016/j.celrep.2019.07.060
66. Sivapathasuntharam C, Hayes MJ, Shihmar H, Kam JH, Sivaprasad S, Jeffery G. Complement factor H regulates retinal development and its absence may establish a footprint for age related macular degeneration. *Sci Rep.* (2019) 9:1082. doi: 10.1038/s41598-018-37673-6
67. Chen M, Muckersie E, Robertson M, Forrester JV, Xu H. Up-regulation of complement factor B in retinal pigment epithelial cells is accompanied by complement activation in the aged retina. *Exp Eye Res.* (2008) 87:543–50. doi: 10.1016/j.exer.2008.09.005
68. Cheng X, He D, Liao C, Lin S, Tang L, Wang YL, et al. IL-1/IL-1R signaling induced by all-trans-retinal contributes to complement alternative pathway activation in retinal pigment epithelium. *J Cell Physiol.* (2021) 236:3660–74. doi: 10.1002/jcp.30103
69. Leinphase I, Rozanski M, Harhausen D, Thurman JM, Schmidt OI, Hossini AM, et al. Inhibition of the alternative complement activation pathway in traumatic brain injury by a monoclonal anti-factor B antibody: a randomized placebo-controlled study in mice. *J Neuroinflammation.* (2007) 4:13. doi: 10.1186/1742-2094-4-13
70. Alawieh A, Langley EF, Weber S, Adkins D, Tomlinson S. Identifying the role of complement in triggering neuroinflammation after traumatic brain injury. *J Neurosci.* (2018) 38:2519–32. doi: 10.1523/JNEUROSCI.2197-17.2018
71. Ma W, Cococar R, Gotoh N, Gieser L, Villasmil R, Cogliati T, et al. Gene expression changes in aging retinal microglia: relationship to microglial support functions and regulation of activation. *Neurobiol Aging.* (2013) 34:2310–21. doi: 10.1016/j.neurobiolaging.2013.03.022
72. Leinphase I, Holers VM, Thurman JM, Harhausen D, Schmidt OI, Pietzcker M, et al. Reduced neuronal cell death after experimental brain injury in mice lacking a functional alternative pathway of complement activation. *BMC Neurosci.* (2006) 7:55. doi: 10.1186/1471-2202-7-55
73. Nataf S, Carroll SL, Wetsel RA, Szalai AJ, Barnum SR. Attenuation of experimental autoimmune demyelination in complement-deficient mice. *J Immunol.* (2000) 165:5867–73. doi: 10.4049/jimmunol.165.10.5867
74. Wilson WA, Hughes GR, Lachmann PJ. Deficiency of factor B of the complement system in sickle cell anaemia. *Br Med J.* (1976) 1:367–9. doi: 10.1136/bmj.1.6006.367
75. Coan PM, Barrier M, Alfazema N, Carter RN, Marion de Procé S, Dopico XC, et al. Complement factor B is a determinant of both metabolic and cardiovascular features of metabolic syndrome. *Hypertension.* (2017) 70:624–33. doi: 10.1161/HYPERTENSIONAHA.117.09242
76. Broders-Bondon F, Paul-Gilloteaux P, Gazquez E, Heysch J, Piel M, Mayor R, et al. Control of the collective migration of enteric neural crest cells by the complement anaphylatoxin C3a and N-cadherin. *Dev Biol.* (2016) 414:85–99. doi: 10.1016/j.ydbio.2016.03.022
77. Carmona-Fontaine C, Theveneau E, Tzekou A, Tada M, Woods M, Page KM, et al. Complement fragment C3a controls mutual cell attraction during collective cell migration. *Dev Cell.* (2011) 21:1026–37. doi: 10.1016/j.devcel.2011.10.012
78. Locher H, de Groot JC, van Iperen L, Huisman MA, Frijns JH, de Sousa C, et al. Distribution and development of peripheral glial cells in the human fetal cochlea. *PLoS One.* (2014) 9:e88066. doi: 10.1371/journal.pone.0088066
79. Wang SJ, Furusho M, D'Sa C, Kuwada S, Conti L, Mores DK, et al. Inactivation of fibroblast growth factor receptor signaling in myelinating glial cells results in significant loss of adult spiral ganglion neurons accompanied by age-related hearing impairment. *J Neurosci Res.* (2009) 87:3428–37. doi: 10.1002/jnr.22164
80. Jeon EJ, Xu N, Xu L, Hansen MR. Influence of central glia on spiral ganglion neuron neurite growth. *Neuroscience.* (2011) 177:321–34. doi: 10.1016/j.neuroscience.2011.01.014
81. Mao Y, Reiprich S, Wegner M, Fritzsche B. Targeted deletion of Sox10 by Wnt1-cre defects neuronal migration and projection in the mouse inner ear. *PLoS One.* (2014) 9:e94580. doi: 10.1371/journal.pone.0094580

82. Hibino H, Higashi-Shingai K, Fujita A, Iwai K, Ishii M, Kurachi Y. Expression of an inwardly rectifying K⁺ channel, Kir5.1, in specific types of fibrocytes in the cochlear lateral wall suggests its functional importance in the establishment of endocochlear potential. *Eur J Neurosci.* (2004) 19:76–84. doi: 10.1111/j.1460-9568.2004.03092.x
83. Ando M, Takeuchi S. Immunological identification of an inward rectifier K⁺ channel (Kir4.1) in the intermediate cell (melanocyte) of the cochlear stria vascularis of gerbils and rats. *Cell Tissue Res.* (1999) 298:179–83. doi: 10.1007/s004419900066
84. Neusch C, Papadopoulos N, Müller M, Maletzki I, Winter SM, Hirrlinger J, et al. Lack of the Kir4.1 channel subunit abolishes K⁺ buffering properties of astrocytes in the ventral respiratory group: impact on extracellular K⁺ regulation. *J Neurophysiol.* (2006) 95:1843–52. doi: 10.1152/jn.00996.2005
85. Rozenfurt N, Lopez I, Chiu CS, Kofuji P, Lester HA, Neusch C. Time course of inner ear degeneration and deafness in mice lacking the Kir4.1 potassium channel subunit. *Hear Res.* (2003) 177:71–80. doi: 10.1016/s0378-5955(02)00799-2
86. Calton MA, Lee D, Sundaresan S, Mendus D, Leu R, Wangsawihardja F, Johnson, K.R., Mustapha M. A lack of immune system genes causes loss in high frequency hearing but does not disrupt cochlear synapse maturation in mice. *PLoS One* (2014);9:e94549, doi: 10.1371/journal.pone.0094549
87. Harboe M, Ulvund G, Vien L, Fung M., Mollnes, T.E. He quantitative role of alternative pathway amplification in classical pathway induced terminal complement activation. *Clin Exp Immuno* (2004);138:439–446. doi: 10.1111/j.1365-2249.2004.02627.x
88. Held K, Thiel S, Loos M, Petry F. Increased susceptibility of complement factor B/C2 double knockout mice and mannan-binding lectin knockout mice to systemic infection with *Candida albicans*. *Mol Immunol.* (2008) 45:3934–41. doi: 10.1016/j.molimm.2008.06.021
89. Taube C, Thurman JM, Takeda K, Joetham A, Miyahara N, Carroll MC, et al. Factor B of the alternative complement pathway regulates development of airway hyperresponsiveness and inflammation. *Proc Natl Acad Sci U S A.* (2006) 103:8084–9. doi: 10.1073/pnas.0602357103
90. McWhorter FY, Wang T, Nguyen P, Chung T, Liu WF. Modulation of macrophage phenotype by cell shape. *Proc Natl Acad Sci U S A.* (2013) 110:17253–8. doi: 10.1073/pnas.1308887110
91. Piao C, Zhang WM, Li TT, Zhang CC, Qiu S, Liu Y, et al. Complement 5a stimulates macrophage polarization and contributes to tumor metastases of colon cancer. *Exp Cell Res.* (2018) 366:127–38. doi: 10.1016/j.yexcr.2018.03.009
92. Amorim A, De Feo D, Friebel E, Ingelfinger F, Anderfuhren CD, Krishnarajah S, et al. IFN γ and GM-CSF control complementary differentiation programs in the monocyte-to-phagocyte transition during neuroinflammation. *Nat Immunol.* (2022) 23:217–28. doi: 10.1038/s41590-021-01117-7
93. Borse V, Kaur T, Hinton A, Ohlemiller K, Warchol ME. Programmed cell death recruits macrophages into the developing mouse cochlea. *Front Cell Dev Biol.* (2021) 9:777836. doi: 10.3389/fcell.2021.777836
94. Song X, Li Y, Guo R, Yu Q, Liu S, Teng Q, et al. Cochlear resident macrophage mediates development of ribbon synapses via CX3CR1/CX3CL1 axis. *Front Mol Neurosci.* (2022) 15:1031278. doi: 10.3389/fnmol.2022.1031278
95. Kaur T, Zamani D, Tong L, Rubel EW, Ohlemiller KK, Hirose K, et al. Fractalkine signaling regulates macrophage recruitment into the cochlea and promotes the survival of spiral ganglion neurons after selective hair cell lesion. *J Neurosci.* (2015) 35:15050–61. doi: 10.1523/JNEUROSCI.2325-15.2015
96. Kaur T, Clayman AC, Nash AJ, Schrader AD, Warchol ME, Ohlemiller KK. Lack of Fractalkine receptor on macrophages impairs spontaneous recovery of ribbon synapses after moderate noise trauma in C57BL/6 mice. *Front Neurosci.* (2019) 13:620. doi: 10.3389/fnins.2019.00620
97. Bedeir MM, Ninoyu Y, Nakamura T, Tsujikawa T, Hirano S. Multiplex immunohistochemistry reveals cochlear macrophage heterogeneity and local auditory nerve inflammation in cisplatin-induced hearing loss. *Front Neurol.* (2022) 13:1015014. doi: 10.3389/fneur.2022.1015014
98. Lang H, Nishimoto E, Xing Y, Brown LN, Noble KV, Barth JL, et al. Contributions of mouse and human hematopoietic cells to remodeling of the adult auditory nerve after neuron loss. *Mol Ther.* (2016) 24:2000–11. doi: 10.1038/mt.2016.174
99. Shi X. Resident macrophages in the cochlear blood-labyrinth barrier and their renewal via migration of bone-marrow-derived cells. *Cell Tissue Res.* (2010) 342:21–30. doi: 10.1007/s00441-010-1040-2
100. Lang H, Noble KV, Barth JL, Rumschlag JA, Jenkins TR, Storm SL, et al. The stria vascularis in mice and humans is an early site of age-related cochlear degeneration, macrophage dysfunction, and inflammation. *J Neurosci.* (2023) 43:5057–75. doi: 10.1523/JNEUROSCI.2234-22.2023
101. Noble KV, Liu T, Matthews LJ, Schulte BA, Lang H. Age-related changes in immune cells of the human cochlea. *Front Neurol.* (2019) 10:895. doi: 10.3389/fneur.2019.00895